Received: April 8, 2023. Revised: May 20, 2023. 11

International Journal of
Intelligent Engineering & Systems

http://www.inass.org/

Blood Vessel Segmentation and Classification for Diabetic Retinopathy Grading Using Dandelion Optimization Algorithm with Deep Learning Model

R. Ramesh[1]* S. Sathiamoorthy[2]

[1]*Department of Computer Application, Government Arts and Science College for Women, Karimangalam, Dharmapuri - 635 111, India*
[2]*Annamalai University PG Extension Centre, Villupuram, India*
* Corresponding author's Email: radha.esh@gmail.com

Abstract: Diabetic retinopathy (DR) is a diabetic complexity that mainly affects the eye. Generally, an ophthalmologist defines the severity of the retinopathy by directly inspecting colour images and estimating them by visually examining the fundus. Due to the enormous amount of diabetic patients all over the world, it becomes an expensive process. The automated system was designed for accurate recognition of the disease using segmentation and fundus image. The blood vessel segmentation process is used to identify and separate blood vessels from the surrounding tissues in an image. This is a crucial stage in the detection of DR, as it enables physicians to measure and identify changes in blood vessels that are indicative of the disease. Numerous approaches are used for blood vessel segmentation and DR classification, along with deep learning (DL) and machine learning (ML) techniques. In this article, we introduce a novel dandelion optimization algorithm with deep learning based blood vessel segmentation and classification (DOADL-BVSC) model for DR grading. The presented DOADL-BVSC technique involves the concepts of blood vessel segmentation and DL-based classification for DR diagnosis on retinal fundus photographs. To accomplish this, the presented DOADL-BVSC technique uses the fuzzy set type-II approach for the image enhancement process. Next, U-Net with Bi-directional feature pyramid network (U-BFPN) model is exploited to segment the blood vessels in the retinal imaging effectively. Moreover, a squeeze and excitation (SE) network is applied for feature vector generation with DOA based hyperparameter optimizer. Finally, quantum autoencoder (QAE) approach is utilized for identifying and classifying DR into distinct stages. The experimental analysis of the DOADL-BVSC approach is investigated on benchmark DR datasets. The simulation results depicted the superior results of the DOADL-BVSC technique with increased accuracy of 99.93%.

Keywords: Diabetic retinopathy, Retinal fundus images, Blood vessel segmentation, Dandelion optimizer, Deep learning.

1. Introduction

Diabetic retinopathy (DR) is a crucial sources of sightlessness amid the labour-age populace. It is also one of the majorly dreaded complexities of diabetic disease [1]. The principal issue of DR is that it develops into an incurable disease in its progressive phases and hence initial diagnosis is very crucial [2]. But this contains a notable struggle in the medical care system because of its tremendous number of possible patients and the lesser number of trained specialists. Physical identification of DR needs greatly proficient medics to accomplish the assessments [3]. Additionally, even greatly trained ophthalmologists get affected by intra- and inter-grader discrepancies. Hence, automatic identification of DR by employing precise ML algorithms has the latent to reduce such inadequacies [4]. This also has inspired the requirement to build an automatic diagnostic structure to help in initial DR diagnosing. Many trials are taken towards this track, and many methods founded on hand-crafted aspects have been suggested [5], which have demonstrated hopeful efficaciousness in perceiving DR areas in the images of the retinal fundus. Hand-crafted factors are generally implemented with conventional ML

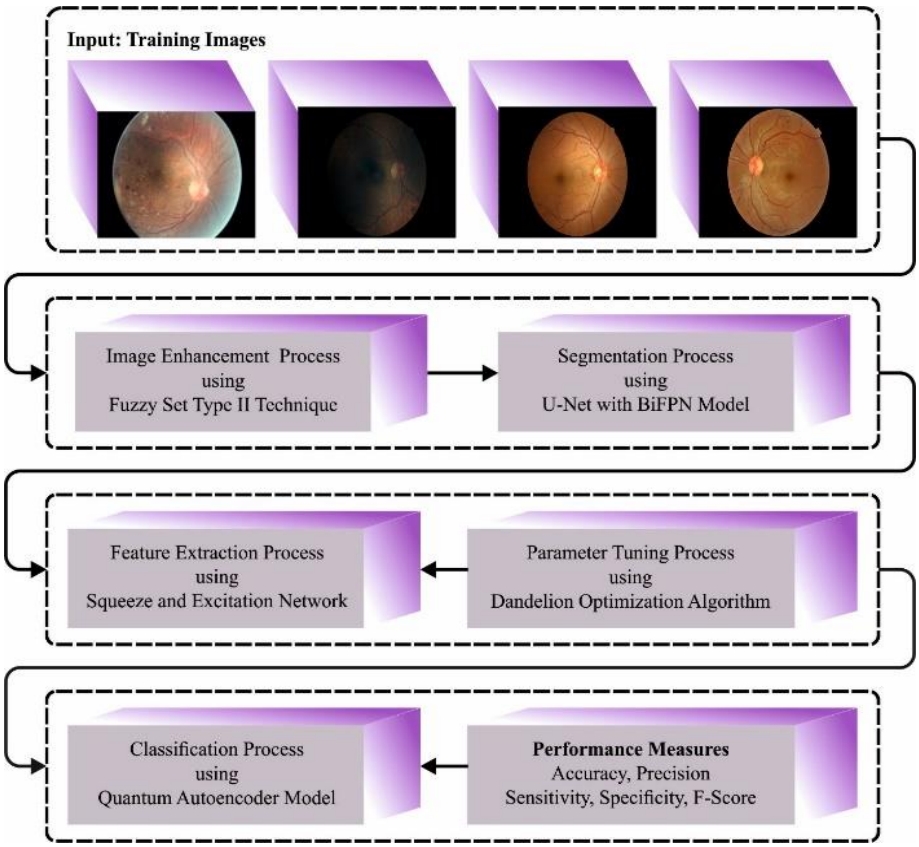

Figure. 1 Overall flow of DOADL-BVSC technique

procedures for the diagnosing of DR [6].

Recently, the accessibility of enormous datasets and the large calculating power presented by graphical processing units (GPU) have inspired experiments on DL methods that have demonstrated extraordinary accomplishment in several tasks of computer vision and have acquired definite success over conventional procedures based on hand-engineering. Several DL-founded procedures are also built for several jobs to evaluate images of the retinal fundus to build automated CAD schemes for DR. To categorize DR, there exist two types of digitalized structures. DL-founded methods accomplished crucially greater precision when associated with factors resulting from implementing convolutional image-processing schemes. However, to avert overfitting with a minimum dataset of HR, certain DL networking should be fine-tuned using metaheuristics such as puzzle optimization algorithm (POA) [7], three influential members based optimizer (TIMBO) [8], guided pelican algorithm (GPA) [9], stochastic komodo algorithm (SKA) [10], etc.

This study presents introduces a novel dandelion optimization algorithm with deep learning based blood vessel segmentation and classification (DOADL-BVSC) model for DR grading. The presented DOADL-BVSC technique uses a fuzzy set type-II approach for the image enhancement process. Next, U-Net with Bi-directional feature pyramid network (U-BFPN) model is exploited to segment the blood vessels in the retinal imaging effectively. Moreover, a squeeze and excitation (SE) network is applied for feature vector generation with DOA based hyperparameter optimizer. Finally, quantum autoencoder (QAE) approach is utilized for identifying and classifying DR into distinct stages. The experimental analysis of the DOADL-BVSC approach is investigated on benchmark DR datasets.

The remaining sections of the paper is arranged as follows. Section 2 offers the literature review and section 3 introduces the proposed model. Then, section 4 elaborates the results analysis and section 5 concludes the work.

2. Literature review

Jena et al. [11] devise a novel technique utilizing an asymmetric DL feature named the new diabetic retinopathy screening approach. Utilizing U-Net for the BVS and optical disc, the asymmetric DL features were derived. For DR lesions classification, a CNN with an SVM has been used. In [12], developed a technique using CNN called potential automatic diabetic recognition in fundus photographs. Initially, the preprocessing phase is accomplished through adaptive histogram equalizations (AHEs) to enrich

the input images. So, CNN and fuzzy C-means clustering (FCMs), exudates segmenting and blood vessel segmenting were done. Later, texture feature was derived from exudates and blood vessels. After the extracting feature, using SVM, the diabetic classification is done.

Kumar et al. [13] designed improved methods for haemorrhages and the detection of microaneurysms, which contribute to the overall enhancement in the initial recognition of DR. The presented technique is composed of 5 different stages they are the localization of fovea, pre-processing, segmenting of the optic disc, classification, feature extracting process and detection of blood vessels. In [14], the author concentrated on the application of different DL approaches for precise retinal vasculature semantic segmentation. The author has exploited 3 distinct methods: CNN, UNet, and SegNet.

In [15], the author implements and designs a DL-related technique for the automated segmenting of the retinal vessel. It would adopt a U-shaped structure comprising a decoder and an encoder using a multi-scale fusion, cross-stage local connectivity system, and attention module, which gain enhanced segmentation outcomes having limited dataset capability. Shankar et al. [16] present an HPTI-v4, a novel automatic Tuning Inception-v4 model for classifying and detecting DR from colour fundus imaging. In the pre-processing phase, using contrast limited adaptive histogram equalization (CLAHE) approach, the contrast level of fundus imaging is improvised. Then, for extracting the essential factors from segmentation images, the HPTI-v4 method was implemented and it undergoes classification using an MLP.

Though several DR diagnosis methods are accessible in the literature, there still exist a requirement for boosting the DR classification achievement. Most of the existing models have not focused on metaheuristic optimization algorithms.

3. The proposed model

In this research, we have focused on the development of the DOADL-BVSC technique for accurate and automated DR diagnosis on retinal fundus images. The DOADL-BVSC technique involves fuzzy set type-II-based image enhancement, U-BFPN blood vessel segmentation, SE network-based feature extracting, DOA-based parameter tuning, and QAE classification. Fig. 1 depicts the comprehensive flow of the DOADL-BVSC model.

3.1 Image enhancement using fuzzy set type-II approach

Primarily, the fuzzy set type-II approach takes place for enhancing the quality of the input images [17]. The preprocessing stage eradicates imperfection from the fundus photographs, enhances the quality of the image, and enables spatial domain technique to be operated on pixels. Along with their efficacy in computation, spatial domain technique requires lesser computational power. The pixel value was directly applied as an input dataset. This enhancement method depends on the grey level to improve the higher contrasted imaging generated by the pixel-dependent model. The spatial domain technique was applied at the preprocessing stage to successfully process the image in the following phase.

$$\mu'(g_{ij}) = \frac{g - g_m}{g_{\max} - g_{\min}} \tag{1}$$

The upper and lower boundaries of the type-II fuzzy member function can be evaluated by the following expression:

The upper membership function,

$$\mu^{upper} = [\mu(x)]^{\alpha} \tag{2}$$

The lower membership function,

$$\mu^{lower} = [\mu(x)]^{\frac{1}{\alpha}}, \propto = 0.9, 0 < \alpha \leq 1 \tag{3}$$

In Eq. (3), $g_{\max}$ and $g_{\min}$ represent the maximal and minimal image colour levels. $\propto$ denotes the image colour level lies within [0,1]. The improved image relies on the value $of \propto$; once the $\propto$ rises, the image contrast to rises. It is feasible to accomplish this goal with high value and membership value, and as a result, the enhanced images can be enhanced. Hamacher T's co-norm was employed for finding the membership values.

$$\mu^{enhanced}(g_{i|}) = \frac{\mu^{upper} + \mu^{lower} + (\lambda - 2).\mu^{upper}.\mu^{lower}}{1 - (1 - \lambda)\mu^{Upper}.\mu^{lower}} \tag{4}$$

Where $\lambda =$ Image average.

3.2 Blood vessel segmentation process using U-BFPN model

To properly recognize the blood vessels, the segmentation process is performed by the U-BFPN model. The U-net includes the layers of input, output, and hidden. The hidden layer is split into upsampling

and downsampling parts, differentiating the decoder and encoder [18]. The upsampling is composed of convolution and de-convolution layers that perform path role extension in the networking and localize pixel points. Downsampling is composed of convolution and pooling layers that perform path-shrinking roles in networking and capturing global data. In other words, the magnitude of input imagery is similar to the output imagery. The downsampling part of the Unet network is applied for extracting the features of an image. After many operations like maximum pooling and convolution, making the shallow layer data is lost. To integrate the low- and high-resolution information better, the study integrates the Bi-FPN with the Unet network for forming a new network architecture. Bi-FPN is applied for replacing the skip connection, and the weight concept is developed for enhancing the efficiency of the model and balancing the featuring data of different scales. The high level of semantic data better helps to accurately segment the target. While performing the downsampling process in deep images, some fine target data can be discarded. The multiscale feature fusion model is a better solution to these problems.

The ReLU procedure is implemented after every ω_i, via $\omega_i \geq 0$ and to retain stability of mathematical value, we set $\varepsilon = 0.0001$ at a smaller value. Furthermore, the exponent function that went under normalization is not executed, and the value of the weight of every normalized parameter is within $[0,1]$.

The neural network model based on U-BFPN extracts blood vessels in a superior way. It exploits Bi-FPN as a featured network and U-net as a backbone network to transmit shallow data. The discrepancy is that the Bi-FPN networking fuses contextual information better in the general framework to prevent poor accuracy of the segmentation.

3.3 Feature extraction

For feature extraction purposes, the SE network is utilized in this work. The SE network is a NN structure which is utilized for extracting features [19]. The SE network was intended to enhance the performance of CNNs with selective highlighting of vital features and suppressing fewer essential ones. The network gains this by utilizing a process termed channel-wise feature recalibration that comprises 2 essential steps: Squeeze: The SE network primarily squeezes the spatial dimensional of every mapping feature as a global descriptor by executing global average pooling. This decreases the parameter counts and computational complexity of networks. Excitation: The network then learns to re-weight the channels of mapping features dependent upon their importance. In particular, it utilizes a small MLP to learn a channel-wise scaling factor which is executed for the mapping feature. The MLP was trained to learn the significance of every channel by utilizing the global descriptor acquired in the squeeze stage. By integrating the SE element as CNN, the network was capable of improving its performance on an extensive range of image classification tasks. The SE network also be utilized in other applications like segmentation, image captioning, and object detection.

For improving the performance of the SE network, the DOA is used for the hyperparameter tuning process. The DOA comprises 3 stages intersected by the dandelion seeds in its lifespan journey such as descending, landing, and rising [20]. Taking the same rule as that meta-heuristic technique simulated naturally, the presented technique was dependent upon initialized of the population with their iterative and evolution optimizer. Certainly, every seed of dandelions is assumed a candidate result. In accordance, the population is defined by the matrix representation (Eq. (5)):

$$Pop = \begin{bmatrix} x_{1,1} & x_{1,2} & \cdots & x_{1,D} \\ x_{2,1} & x_{2,2} & \cdots & x_{2,D} \\ \vdots & \vdots & \ddots & \vdots \\ x_{NP,1} & x_{NP,2} & \cdots & x_{NP,D} \end{bmatrix} \tag{5}$$

whereas, D refers to the variable dimensional. NP defines the population size. Determining 2 boundary bands to preserved problems like upper and lower ones, represented by Ub and Lb correspondingly, as revealed in these formulas:

$$\begin{cases} Ub_j = [u_1, \ldots, ub_D] \\ Lb_j = [lb_1, \ldots, lb_D] \end{cases} \tag{6}$$

In which, j stands for the integer among 1 and NP. Several candidate outcomes were necessarily being created arbitrarily among such boundaries to every individual $X_{i,j}$ is written based on Eq. (7):

$$\chi_{i,j} = Lb_j + rand \cdot \left(Ub_j - Lb_j\right) \tag{7}$$

and denotes the random number between $zero$ and one.

In the initialized procedure, the algorithm begins with selecting the individual taking a better fitness value. After locating it, it can be assumed that the primary elite estimates the better place for the flourishing of dandelion seeds. When the minimum value was selected, primary elite x_{eliie} was

formulated as:

$$\begin{cases} F_{best} = \min\left(F_{obj}(x_{i,j})\right) \\ x_{elite} = x(find(F_{best} = F_{obj}(x_{i,j}))) \end{cases} \quad (8)$$

with find () being 2 equivalent indices.

The dandelion seed increases to a particular height and afterwards starts moving far from its parent. Next, according to moisture features and the strength of the wind, the seeds mount to arbitrary heights based on 2 weather circumstances.

Condition 1:

- During clear days and there is an absence of weather changeability, the speed of the wind was distinguished by that is modelled by logarithmic distribution based on Eq. (9):

$$ln\gamma = N(\mu, \sigma^2)) \quad (9)$$

- During this condition, the broadcast by seeds was remote arbitrarily as a distribution is mostly together the y-axis that triggers the procedure of DOA exploration. During this search region, the diffusion of dandelion seeds is carefully compared with the speed of the wind that controls its dispersion and height. During this effect, the vortices over the seeds are always modified for forcing them to spiral upwardly, based on the subsequent formula:

$$X_{t+1} = X_t + \alpha \cdot v_x \cdot v_y \cdot \ln\gamma \cdot (X_s - X_t) \quad (10)$$

- X_t and X_s represent the place of dandelion seeds and searching space for t iteration number, correspondingly. Thus, the place attained by random was formulated as:

$$X_s = rand(1, \dim)(Ub - Lb) + Lb \quad (11)$$

- It can be essential to declare that lnY refers to the lognormal distribution following the conditions $\sigma^2 = 1$ and $\mu = 0$, and so the mathematical model is explained as:

$$\ln\gamma = \begin{cases} \frac{1}{y\sqrt{2\pi}} \exp\left[-\frac{1}{2\sigma^2}(\ln y)^2\right] & y \geq 0 \\ 0 & y \prec 0 \end{cases} \quad (12)$$

- α refers to the fine-tuning hyperparameter to adjust the searching step length, and y is determined as the uniform dispersion $N(0,1)$. Therefore, α is provided as:

$$\alpha = rand(\,) \times \left(\frac{1}{T^2}t^2 - \frac{2}{T}t + 1\right) \quad (13)$$

- It can be demonstrated that the parameter α performs as a function of iteration counts as a random fluctuation from the range of zero and one, which reduces non-linearly nearby 0. If determining v_x and v_y as dandelion lift coefficients parameters in the outcome of whirlwind activity, then force computation on the variable dimensional is given as follows:

$$\begin{cases} r = \frac{1}{e^{\theta}} \\ v_x = r * \cos\theta \\ u_y = r * \sin\theta \end{cases} \quad (14)$$

In which θ represents the random angle from the interval of $-\pi$ and π.

Condition 2:

- During raining days, the air resisting was enhanced because of maximum humidity, and thus dandelion seed's buoyancy and its height from the space is limited contains the requirement to procedure it in its local proximities, based on the subsequent in Eq. (15):

$$X_{t+1} = X_t \times k \quad (15)$$

- whereas k determines the parameter accountable to set the local searching domain of provided dandelion and that is demonstrated by Eq. (16):

$$\begin{cases} q = \left(\frac{1}{T^2-2T+1}t^2 - \frac{2}{T^2-2T+1}t + 1 + \frac{1}{T^2-2T+1}\right) \\ k = 1 - rand() \times q \end{cases} \quad (16)$$

- During this step, the seeds that are enduring the rising stage are estimated by Eq. (17):

With the careful attention that DOA pays towards the exploration procedure, the descending stage was controlled according to the subsequent study reflected by Eq. (18). The dandelion seed concludes its rising step to a particular distance; begins the stage of consistent descent based on a movement trajectory estimated by Brownian movement. Next, the optimization grows the entire populace to promise ethnicities assuming the average location data then the ascension stage and whole situation to simulate the stability of the dandelion descending:

$$X_{t+1} = \begin{cases} X_t + \alpha \times v_x \times v_y \times \ ln\gamma \times (X_s - X_t) rand() < 1.5 \\ X_t \times k \qquad\qquad\qquad\qquad else \end{cases} \quad (17)$$

$$X_{t+1} = X_t - \alpha \times \beta_t \times \left(X_{mean_t} - \alpha \times \beta_t \times X_t\right) \quad (18)$$

In which, β_t implies the arbitrarily created number proceeded in the well-known standard normal distribution and signifies Brown's motion. In the i^{th} iteration, X_{mean_t} stands for the average population place based on Eq. (19):

$$X_{mean_{-i}} = \frac{1}{pop} \sum_{i=1}^{pop} X_i \quad (19)$$

The main to the proper execution of meta-heuristic techniques is the balance among the 2 essential search processes exploitation and exploration. During this case, the DOA efforts, under exploitation, to improve solutions previously acquired in the exploration, for improving its fitness function by examining the neighbouring promising area. As the iterating's proceed, this technique will be converging towards a globally optimum solution that determines the estimated location which makes sure the dandelion seeds are germinated and remain their lifespan through the borrow of the most significant data in actual elite by searching agents for exploiting in its local neighbourhoods. In case, for the i^{th} iteration, X_{elite} signifies the seed optimum position, the equivalent scientific model is written as:

$$X_{t+1} = X_{elite} + levy(\lambda) \times \alpha \times (X_{elite} - \delta \times X_t) \quad (20)$$

In which, levy (λ) refers to the Levy flight function provided as:

$$levy\ (\lambda) = s \times \frac{w \times \sigma}{|t|^{\frac{1}{\beta}}} \quad (21)$$

The parameter β is selected arbitrarily to equivalent 1.5, but s is set at 0.01. w and t are numbered from the interval of zero and one. Consequently, σ is a mathematical model written by:

$$\sigma = \left(\frac{\Gamma(1+\beta) \times \sin\left(\frac{\pi\beta}{2}\right)}{\Gamma\left(\frac{1+\beta}{2}\right) \times \beta \times 2^{\left(\frac{\beta-1}{2}\right)}} \right) \quad (22)$$

According to the preceding value of β, σ enhances linearly follows Eq. (23):

$$\delta = \frac{2t}{T} \quad (23)$$

Algorithm 1 summarizes the pseudocode of the presented DOA technique for PEMFC parameters estimation.

Algorithm 1: Pseudocode of the proposed DOA optimizer

Initializing the primary dandelion seeds population from the arbitrary way
Compute the dandelion seed's fitness values f
Select X_{elite} dependent upon fitness value f
while ($t < T$) do
$if(rand\ () < 1.5)$ then
Create adaptive parameters utilizing Eq. (13)
Upgrade dandelion seeds by Eq. (10)
adaptive parameters utilizing Eq. (16)
Upgrade seeds by Eq. (15)
Upgrade seeds by Eq. (18)
Upgrade seeds by Eq. (20)
Order dandelion seeds dependent upon fitness values
Upgrade X_{elite}
$if\ (f_{elite} = f(X_{best}))$ then
$X_{Best} = X_{elite}, f_{Best} = f(X_{elite})$
Return X_{Best} and F_{best}

Choosing the fitness function is a main aspect of the DOA technique. Solution encoding was employed for evaluating the aptitude of the solution candidate. In this, the precision value was the crucial state employed for constructing a fitness function.

$$Fitness\ =\ \max(P) \quad (24)$$

$$P = \frac{TP}{TP+FP} \quad (25)$$

Where TP and FP signify the true positive and false positive values.

3.4 DR grading

At the final stage, the DR grading and classification process is performed with the use of the QAE model. Autoencoder (AE) is a NN model trained for learning compressed depictions for the series of datasets in an unsupervised way [21]. Firstly, a decreased encoding was generated for the input dataset. Next, the original input was recreated from the decreased encoding. It especially, objects to learning an identity function under certain limitations, for instance, with the constraint amount of neurons in

the concealed layer. The AE includes encoded and decoded parts.

The encoder map the input $x \in Rn$ to the hidden space and, by considering FFNN, the resultant h^{l+1} of the lth layer is formulated by:

$$h_d^{l+1} = \sigma\left(W_e^l \cdot h_e^{(l)}\right) \quad (26)$$

In Eq. (26), W_e^l denotes the trained layer weight and σ represents a nonlinear activation function. Consider the encoded part with he layers, thus $h_e^{(0)} = x$ and tha $t\, h^{(Le)} = h$, where $h \in Rk$ denotes the compressed version.

The decoder, rather, map the h compressed representation back towards the original space and, by taking an FFNN into cannot, we have that:

$$h_d^{(l+1)} = \sigma(W_d^{(l)}) \cdot (h_d^{(l)}) \quad (27)$$

In Eq. (27), $h_d^{(l+1)}$ denotes the resultant of $the\ lth$ layer, W_d represents the trained weight matrix and σ represents a nonlinear activation function. Consider L_d layers, thus $h_d^{(0)} = h$ and that $h^{(L_d)} + x'$, where x' shows the regeneration of input vector x.

The objective of AE is to recreate the input $(ideally\ x' = x)$, it is trained by minimalizing the reconstructed error $(x', x) = x' - x$, represented as a loss function, through the BP model.

Note that, other neural architectures, unlike FFNN, are regarded as encoded or decoded parts based on a certain application with an arbitrary amount of hidden layers. Quantum ML largely handles extending traditional ML issues to the quantum domain with variating quantum circuiting [22]. The circuit can be divided into three different blocks; measurement and post-processing parts that calculate the evolving state and process the obtained observable further, and a state preparation encodes conventional input into a quantum state. We often work in the computation base with the basis vector $\{|0\rangle, |1\rangle\}$ representing the eigenstate of the Pauli Z operator σ_z for all the qubits. There exist several examples of state preparation that has own advantages in different applications. The state is prepared through angle encoding that encodes real-valued observable ϕ_j as rotation angle alongside the x-axis of the Bloch sphere.

$$|\Phi\rangle = \otimes_{i=1}^{n} R_x\left(\phi_j\right)|0\rangle = \otimes_{j=1}^{n}(\cos\frac{\phi_j}{2}|0\rangle - i\sin\frac{\phi_j}{2}|1\rangle), \quad (28)$$

In Eq. (28), $R_x = e^{-i\frac{\phi_j}{2}\hat{\sigma}_x}$ represent the rotational matrices. The amount of qubits needed n, is identical to the dimension of the input vector. A parametrized unitary circuit (Θ), with Θ representing the parameter set, evolving the prepared state $|\Phi\rangle$ to the concluding state $|\Psi\rangle$,

$$|\Psi\rangle = U(\Theta)|\Phi\rangle. \quad (29)$$

The last stage includes the observable measurement of the concluding state $|\Psi\rangle$. Meanwhile, measurement in quantum mechanics is intrinsically probabilistic, we evaluate different times (named shots) to obtain a precise outcome.

For this purpose, quantum hardware is needed that could prepare a massive amount of input states $|\Phi\rangle$ for every data point.

Afterwards determining the cost function, the parameter Θ is trained and upgraded utilizing the optimization technique.

4. Results analysis

In this segment, the DR classification results of the DOADL-BVSC technique are studied on the DR database from Kaggle repositories [23]. The dataset comprises 35126 samplings with five classes as shown in Table 1. Fig. 2 represents the sample images.

The confusion matrix of the DOADL-BVSC approach to the DR classifying process is given in Fig. 3.

Table 2 report comprehensive DR classifying outputs of the DOADL-BVSC model on different

Table 1. Details of dataset

Label	Class	No. of Instances
DR-0	No DR	25810
DR-1	Mild DR	2443
DR-2	Moderate DR	5292
DR-3	Severe DR	873
DR-4	Proliferative DR	708
Total No. of Instances		**35126**

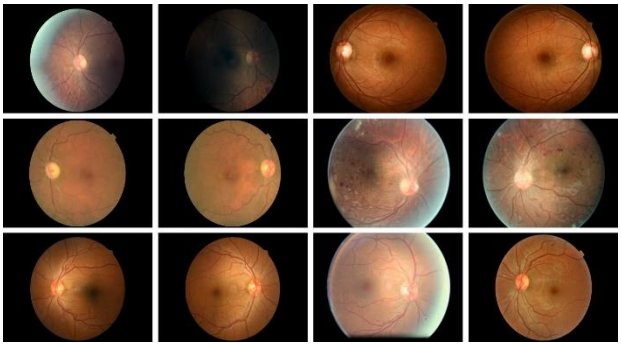

Figure. 2 Sample images

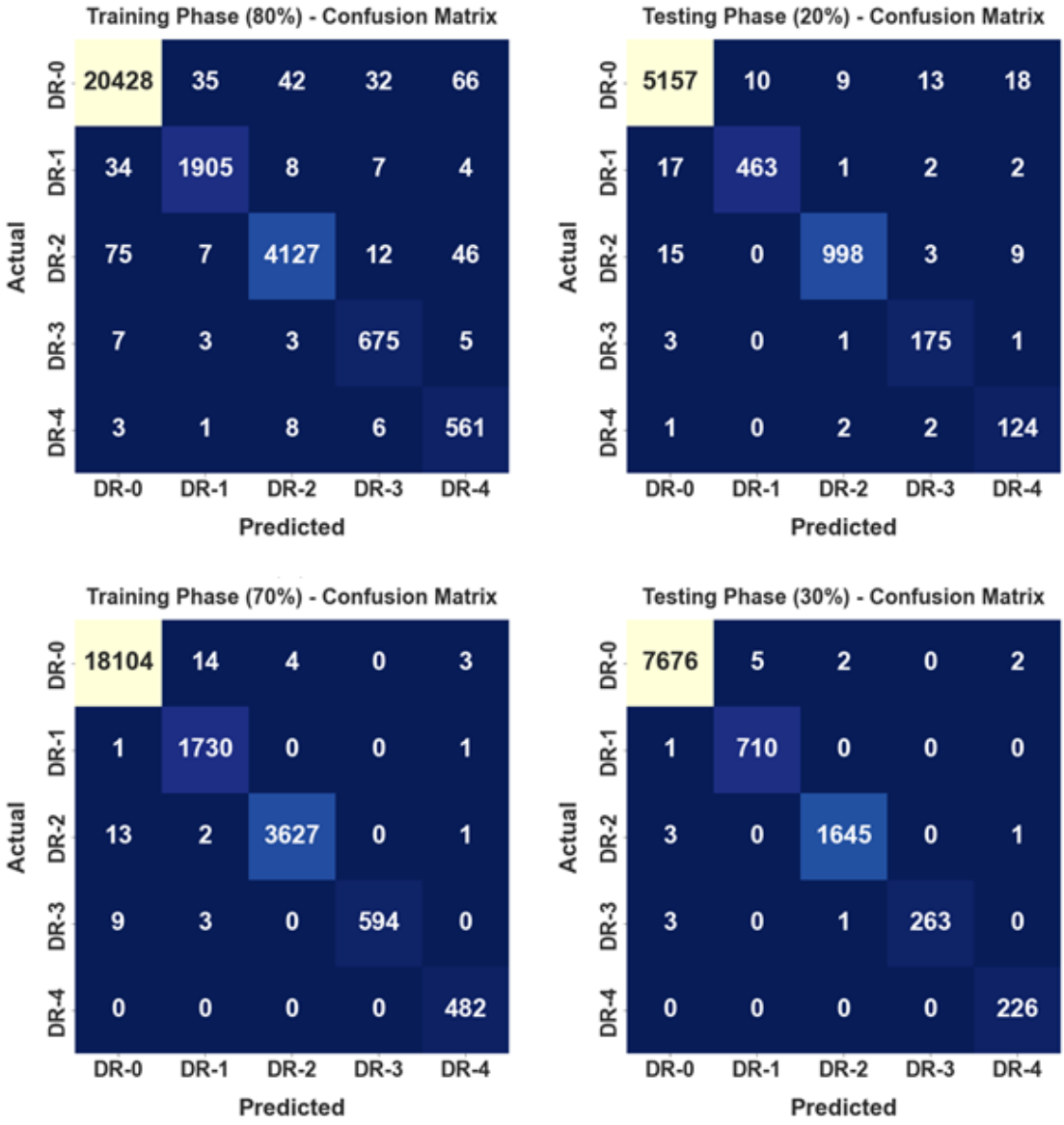

Figure. 3 Confusion matrices of proposed model

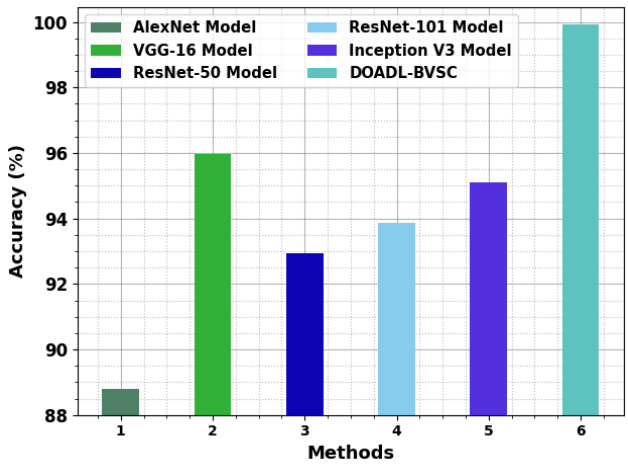

Figure. 4 $Accu_y$ outcomes of the DOADL-BVSC method with other approaches

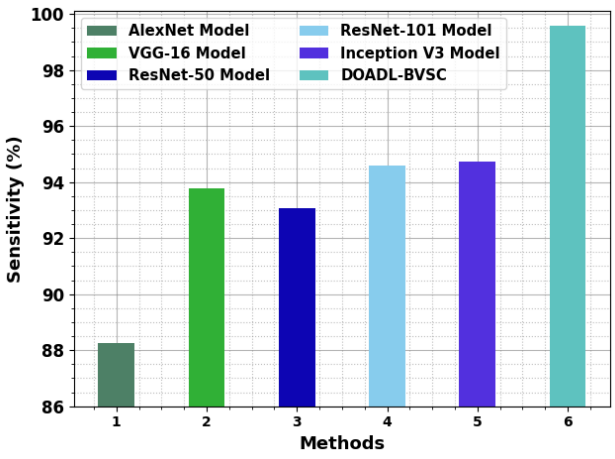

Figure. 5 $Sens_y$ outcomes of the DOADL-BVSC method with other approaches

Table 2. DR classifier outcome of DOADL-BVSC approach under distinct TRP and TSP

Class	$Accu_y$	$Prec_n$	$Sens_y$	$Spec_y$	F_{score}
Training Phase (80%)					
0-DR	98.95	99.42	99.15	98.41	99.29
1-DR	99.65	97.64	97.29	99.82	97.47
2-DR	99.28	98.54	96.72	99.74	97.62
3-DR	99.73	92.21	97.40	99.79	94.74
4-DR	99.51	82.26	96.89	99.56	88.98
Average	**99.42**	**94.02**	**97.49**	**99.47**	**95.62**
Testing Phase (20%)					
0-DR	98.78	99.31	99.04	98.02	99.17
1-DR	99.54	97.89	95.46	99.85	96.66
2-DR	99.43	98.71	97.37	99.78	98.04
3-DR	99.64	89.74	97.22	99.71	93.33
4-DR	99.50	80.52	96.12	99.57	87.63
Average	99.38	93.23	97.04	99.38	94.97
Class	**$Accu_y$**	**$Prec_n$**	**$Sens_y$**	**$Spec_y$**	**F_{score}**
Training Phase (70%)					
0-DR	99.82	99.87	99.88	99.64	99.88
1-DR	99.91	98.91	99.88	99.92	99.40
2-DR	99.92	99.89	99.56	99.98	99.73
3-DR	99.95	100.00	98.02	100.00	99.00
4-DR	99.98	98.97	100.00	99.98	99.48
Average	**99.92**	**99.53**	**99.47**	**99.90**	**99.50**
Testing Phase (30%)					
0-DR	99.85	99.91	99.88	99.75	99.90
1-DR	99.94	99.30	99.86	99.95	99.58
2-DR	99.93	99.82	99.76	99.97	99.79
3-DR	99.96	100.00	98.50	100.00	99.25
4-DR	99.97	98.69	100.00	99.97	99.34
Average	**99.93**	**99.54**	**99.60**	**99.93**	**99.57**

sizes of TRP and TSP. The results indicate the proficient ability of the DOADL-BVSC technique in the DR classification process.

A comparative result of the DOADL-BVSC technique on DR grading is reported in Fig. 4. The figure highlights comparative research of the DOADL-BVSC method in terms of $accu_y$. 5 Meanwhile, the VGG-16 and Inception v3 methods have portrayed sensible $accu_y$ of 95.98% and 95.10%. Nevertheless, the DOADL-BVSC technique resulted in a maximum $accu_y$ of 99.93%.

Fig. 5 highlighted a relative study of the DOADL-BVSC approach in terms of $sens_y$. The figure showed that the AlexNet technique reaches least $sens_y$ of 88.26% while the ResNet-50 and ResNet-101 approaches have gained closer $sens_y$ values of 93.07% and 94.61% respectively. Nevertheless, the DOADL-BVSC method resulted in a maximal $sens_y$ of 99.60%.

5. Conclusion

In this article, we have focused on the development of the DOADL-BVSC technique for accurate and automated DR diagnosis on retinal fundus images. The DOADL-BVSC technique involves fuzzy set type-II-based image enhancement, U-BFPN blood vessel segmentation, Squeeze and excitation network-based feature extracting process, DOA-based tuning process, and QAE classification. The experimental analysis of the DOADL-BVSC approach is examined on benchmark DR datasets. In the upcoming years, the detection performance of the DOADL-BVSC algorithm can be boosted by voting classification models.

Conflict of interest

The authors declare no conflict of interest.

Author contributions

Conceptualization, Ramesh and Sathiamoorthy; methodology, Ramesh and Sathiamoorthy; software, Ramesh; validation, Ramesh; formal analysis, Ramesh and Sathiamoorthy; investigation, Ramesh and Sathiamoorthy; resources, Ramesh; data curation, Ramesh; writing-original draft preparation, Ramesh; writing-review and editing, Ramesh and Sathiamoorthy; visualization, Ramesh; supervision, Ramesh; project administration, Ramesh; funding acquisition, Ramesh. All authors have read and approved the final manuscript.

References

[1] G. T. Reddy, S. Bhattacharya, S. S. Ramakrishnan, C. L. Chowdhary, S. Hakak et al., "An Ensemble based Machine Learning model for Diabetic Retinopathy Classification", In: *Proc. of 2020 International Conference on Emerging Trends in Information Technology and Engineering (ic-ETITE)*, Vellore, India, pp. 1-6, 2020, doi: 10.1109/ic-ETITE47903.2020.235.

[2] D. Qomariah, I. T. S. Nopember, H. Tjandrasa, and C. Fatichah, "Segmentation of Microaneurysms for Early Detection of Diabetic Retinopathy Using MResUNet", *International Journal of Intelligent Engineering and Systems*, Vol. 14, No. 3, 2021, doi: 10.22266/ijies2021.0630.30.

[3] M. Pundikal and M. S. Holi, "Detection of Microaneurysms Using Grey Wolf Optimization for Early Diagnosis of Diabetic Retinopathy", *International Journal of Intelligent Engineering and Systems*, Vol. 13, No. 6, pp. 208-218, 2020.

[4] N. S. Basavaraju and S. Ganesarathinam, "Early

Detection of Diabetic Retinopathy Using K-means Clustering Algorithm and Ensemble Classification Approach", *International Journal of Intelligent Engineering and Systems*, Vol. 14, No. 6, 2021, doi: 10.22266/ijies2021.1231.43.

[5] A. Desiani, "BVU-Net: A U-Net Modification by VGG-Batch Normalization for Retinal Blood Vessel Segmentation", *International Journal of Intelligent Engineering and Systems*, Vol. 15, No. 6, 2022, doi: 10.22266/ijies2022.1231.29.

[6] J. G. R. Elwin, J. Mandala, B. Maram, and R. R. Kumar, "Ar-HGSO: Autoregressive-Henry Gas Sailfish Optimization enabled deep learning model for diabetic retinopathy detection and severity level classification", *Biomedical Signal Processing and Control*, Vol. 77, p. 103712, 2022.

[7] F. A. Zeidabadi and M. Dehghani, "POA: Puzzle Optimization Algorithm", *International Journal of Intelligent Engineering and Systems*, Vol. 15, No. 1, 2022, doi: 10.22266/ijies2022.0228.25.

[8] F. A. Zeidabadi, M. Dehghani, and O. P. Malik, "TIMBO: Three Influential Members Based Optimizer", *International Journal of Intelligent Engineering and Systems*, Vol. 14, No. 5, 2021, doi: 10.22266/ijies2021.1031.12.

[9] P. D. Kusuma and M. Kallista, "Guided Pelican Algorithm", *International Journal of Intelligent Engineering and Systems*, Vol. 15, No. 6, 2022, doi: 10.22266/ijies2022.1231.18.

[10] P. D. Kusuma and M. Kallista, "Stochastic Komodo Algorithm", *International Journal of Intelligent Engineering and Systems*, Vol. 15, No. 4, 2022, doi: 10.22266/ijies2022.0831.15.

[11] P. K. Jena, B. Khuntia, C. Palai, M. Nayak, T. K. Mishra et al., "A Novel Approach for Diabetic Retinopathy Screening Using Asymmetric Deep Learning Features", *Big Data and Cognitive Computing*, Vol. 7, No. 1, p. 25, 2023.

[12] C. Raja and L. Balaji, "An automatic detection of blood vessel in retinal images using convolution neural network for diabetic retinopathy detection", *Pattern Recognition and Image Analysis*, Vol. 29, pp. 533-545, 2019.

[13] S. Kumar, A. Adarsh, B. Kumar, and A. K. Singh, "An automated early diabetic retinopathy detection through improved blood vessel and optic disc segmentation", *Optics & Laser Technology*, Vol. 121, p. 105815, 2020.

[14] Z. A. Elaouaber, A. Feroui, M. E. A. Lazouni, and M. Messadi, "Blood vessel segmentation using deep learning architectures for aid diagnosis of diabetic retinopathy", *Computer Methods in Biomechanics and Biomedical Engineering: Imaging & Visualization*, pp. 1-15, 2022, doi: 10.1080/21681163.2022.2145999 .

[15] R. Liu, S. Gao, H. Zhang, S. Wang, L. Zhou et al., "MTNet: A combined diagnosis algorithm of vessel segmentation and diabetic retinopathy for retinal images", *Plos one*, Vol. 17, No. 11, 2022.

[16] K. Shankar, Y. Zhang, Y. Liu, L. Wu, and C. H. Chen, "Hyperparameter Tuning Deep Learning for Diabetic Retinopathy Fundus Image Classification", *IEEE Access*, Vol. 8, pp. 118164-118173, 2020, doi: 10.1109/ACCESS.2020.3005152.

[17] U. Bhimavarapu and G. Battineni, "Deep Learning for the Detection and Classification of Diabetic Retinopathy with an Improved Activation Function", *Healthcare*, Vol. 11, p. 97, 2022.

[18] K. Ren, L. Chang, M. Wan, G. Gu, and Q. Chen, "An improved U-net based retinal vessel image segmentation method", *Heliyon*, Vol. 8, No. 10, 2022.

[19] J. Zhang, P. Ma, T. Jiang, X. Zhao, W. Tan et al., "SEM-RCNN: a squeeze-and-excitation-based mask region convolutional neural network for multi-class environmental microorganism detection", *Applied Sciences*, Vol. 12, No. 19, p. 9902, 2022.

[20] R. Abbassi, S. Saidi, A. Abbassi, H. Jerbi, M. Kchaou et al., "Accurate Key Parameters Estimation of PEMFCs' Models Based on Dandelion Optimization Algorithm", *Mathematics*, Vol. 11, No. 6, p. 1298, 2023.

[21] E. S. Miele, F. Bonacina, and A. Corsini, "Deep anomaly detection in horizontal axis wind turbines using graph convolutional autoencoders for multivariate time series", *Energy and AI*, Vol. 8, p. 100145, 2022.

[22] V. S. Ngairangbam, M. Spannowsky, and M. Takeuchi, "Anomaly detection in high-energy physics using a quantum autoencoder", *Physical Review D*, Vol. 105, No. 9, p. 095004, 2022.

[23] https://www.kaggle.com/competitions/diabetic-retinopathy-detection/overview

[24] G. U. Nneji, J. Cai, J. Deng, H. N. Monday, Hossin, M. A. Nahar et.al, "Identification of Diabetic Retinopathy Using Weighted Fusion Deep Learning Based on Dual-Channel Fundus Scans", *Diagnostics* 2022, Vol. 12, No. 540, doi:10.3390/diagnostics12020540